Phase formation in colloidal systems with tunable interaction

Hauke Carstensen,[*] Vassilios Kapaklis, and Max Wolff

Department of Physics and Astronomy, Uppsala University, Box 516, SE-751 20 Uppsala, Sweden

Self-assembly is one of the most fascinating phenomena in nature and is one key component in the formation of hierarchical structures. The formation of structures depends critically on the interaction between the different constituents, and therefore the link between these interactions and the resulting structure is fundamental for the understanding of materials. We have realized a two-dimensional system of colloidal particles with tunable magnetic dipole forces. The phase formation is studied by transmission optical microscopy and a phase diagram is constructed. We report a phase transition from hexagonal to random and square arrangements when the magnetic interaction between the individual particles is tuned from antiferromagnetic to ferrimagnetic.

I. INTRODUCTION

The formation of ordered structures on all length scales [1] is one of the most fascinating phenomena in nature. As an example, hadrons are composed of elementary particles while galaxies contain billions of stars. Both can be described as processes of self-assembly but they are driven by forces acting on totally different length scales. In the case of elementary particles and galaxies these are the strong and gravitational forces, respectively.

For the formation of condensed matter, mainly electromagnetic forces acting on intermediate length scales are relevant [2]. A highly interesting class of materials for studying the physics involved in the process of phase formation is formed by colloidal systems. These are composed of small particles, with sizes in the nano- to micrometer range, dispersed in a liquid. The big advantage of this approach is that the particles' properties (e.g., size, shape, or composition) can be specifically tailored. As a result the interaction between them becomes well defined and controlled, and as a consequence systems interacting via dipole [3,4], entropic [3], electric [4–6], or magnetic [7–13] forces have been studied and a wide variety of self-assembled structures exhibiting complex phase diagrams have been reported.

For a colloidal system the liquid matrix can be treated as a continuum, since the particles are much larger than the solvent molecules. If now the material properties of the matrix are altered, the interaction between the colloidal particles becomes continuously tunable. This idea was, e.g., realized to adjust the interaction between micrometer-sized charged particles by adding salt to the solvent [14]. A similar approach is possible for magnetic systems. In this case the magnetic susceptibility of the solvent is adjusted by adding magnetic nanoparticles. These are still much smaller than the colloidal particles, and the assumption of a continuous matrix holds. Originally, this idea was put forward in the 1980s [15] and crystalline as well as chain structures were observed [16,17]. If magnetic and nonmagnetic particles are dispersed in a magnetic liquid, the coupling between the respective particles can be tuned from antiferromagnetic to ferrimagnetic, and as a result the phase diagram in an applied magnetic field becomes extremely

rich [8,18]. In this context, Alert *et al.* have shown that on templated surfaces landscape-inversion phase transitions can be studied with respect to particle density by applying an external field [12].

In this paper we present a system that is based on the same mechanism. However, instead of a templated surface the susceptibility of the magnetic matrix is tuned continuously and the coupling between particles changes from antiferromagnetic to ferrimagnetic. Microscopy is used to study the local ordering in a two-dimensional system of colloidal particles. We show that for an in-plane magnetic field polystyrene spheres with two distinct magnetic susceptibilities undergo a phase transition from hexagonal to square ordering on inversion of the energy landscape for one of the particles. We quantitatively characterize the phase transition and explain the experimental results in terms of the changing dipolar interaction.

II. METHODS

The transmission optical microscopy setup used for the present study is sketched in Fig. 1. The liquid is confined in the vertical direction by two glass slides. A ring-shaped spacer with a thickness of 25 μm defines the distance between the slides, confines the polystyrene beads of 10 μm diameter in two dimensions, and seals the sample in the horizontal direction. A pair of coils is used to create a homogeneous in-plane magnetic field.

The ferrofluid (FF) is a water-based dispersion of magnetite (Fe_3O_4, as measured by x-ray diffraction) nanoparticles and was purchased from LiquidResearch. The particles are encapsulated in a layer of carboxylic acid and their concentration in the samples ranges from $\rho_{vol} = 0.1\%$ to 1.3%. The FF susceptibility can be calculated from the bulk susceptibility of Fe_3O_4, which is $\chi_{Fe_3O_4} = 21$ [7], and is in the range of $\chi_f = 0.02$–0.25 in the samples. Two types of polystyrene beads with a nominal diameter of 10 μm were purchased from MicroParticles and added to the FF. The first type of particle has a magnetite shell and shows a superparamagnetic behavior. The susceptibility χ_m of these particles can be derived from the experiment and is given by $\chi_m = \chi_f(\rho_{vol} = 0.72\%) \approx 0.15$. The second type of particle is identical to the first one but without the magnetite shell. However, measurement of the distances between closest neighbors in microscope images reveals that the effective size of the beads slightly changes

———————
[*]hauke.carstensen@physics.uu.se
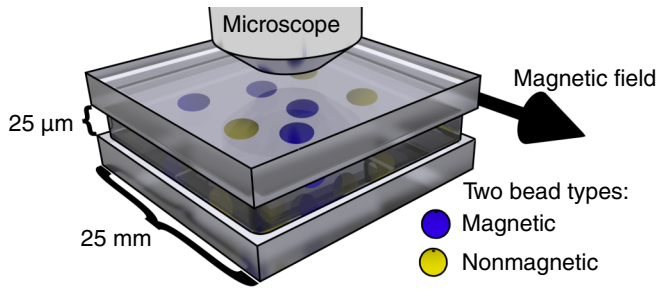
FIG. 1. (Color online) The ferrofluid with suspended magnetic and nonmagnetic beads is framed by two glass slides. The distance between the slides is defined by ring-shaped spacers in such a way that the beads can arrange only in two dimensions. An external magnetic field is applied along the in-plane direction.

depending on the particle interactions, and the particles with magnetite shells appear up to 7% larger than the nonmagnetic ones.

In the transmission microscope pictures, the two particles are discriminated by their different extinction properties for blue ($\lambda = 460$ nm) light, which is larger for the magnetic particles containing a magnetite shell. As a result, in the pictures the magnetic particles appear darker than the nonmagnetic ones. First, equal numbers of polystyrene magnetic and nonmagnetic beads were dispersed in the magnetic liquid with different concentrations of magnetite nanoparticles. Each sample was subjected to an in-plane magnetic field of 20 mT for 15 min until the structure became stable. Before applying the constant magnetic field the field was periodically switched on and off to increase the mobility of the beads.

Figure 2 depicts a microscope image taken with a CCD camera. Each type of particle forms chains along the magnetic field lines. Neighboring chains form a structure and the lattice depends on the particle interaction. For low FF susceptibility $\chi_f/\chi_m < 1$, both hexagonal and square arrangements are found depending on whether the two chains consist of one or two kinds of particles [see Fig. 2(a). For high FF susceptibility $\chi_f/\chi_m > 1$ only the hexagonal lattice is observed [see Fig. 2(b).

For quantitative analysis the images are analyzed by detecting the beads automatically and calculating the distances between pairs. In order to exclude systematic errors, images with area density of beads $\rho_{area} < 4.4\%$ and $\rho_{area} > 44\%$
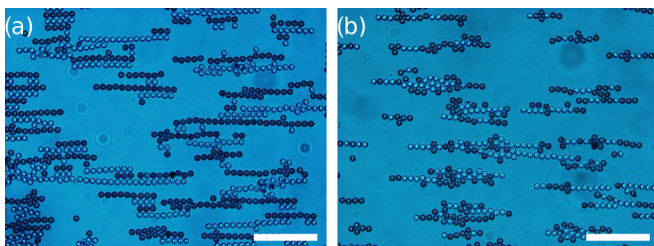
are omitted in our evaluation. For very low bead densities the beads are isolated and do not form clusters, while for very high densities the beads are jammed and do not reach equilibrium positions. The distribution of distances is the pair correlation function and is evaluated for the case where one bead is magnetic and the other one is nonmagnetic. Different lattices can be distinguished by characteristic distances. While in every case the distance between nearest neighbors is equal to the bead diameter a, the distances to the second-nearest neighbors are characteristic for different lattices. For a square arrangement this is the diagonal with the length $d_S = \sqrt{2}a$ and for a hexagonal arrangement this is $d_H = \sqrt{3}a$.

III. RESULTS

Figure 3 depicts the pair correlation function plotted versus the particle diameter or distance between nearest neighbors.

The first and highest peak corresponds to two particles in contact with each other. For larger distances the characteristic distances of the square and hexagonal arrangements show clear peaks. The square peak is more pronounced for small susceptibilities of the FF whereas the hexagonal one is predominant for large susceptibilities. The order parameter for each arrangement can be defined by the amplitudes of the respective peaks in the correlation function.

Additionally, an angular distribution function can be calculated. For one bead that has two or more nearest neighbors the angle between the neighbors can be evaluated. An angle of $60°$ or $120°$ is characteristic for a hexagonal lattice and $90°$ for a square lattice. Chains of beads, isolated or within a cluster, have angles of $180°$.

Figure 4 depicts the intensities at the characteristic values of (a) the pair correlation function and (b) the angular distribution plotted versus the susceptibility of the solvent.

(a)   (b)

FIG. 2. (Color online) Microscope image with (a) $\chi_f/\chi_m = 0.5$ and (b) $\chi_f/\chi_m \approx 1.67$. Magnetic beads (dark) and nonmagnetic beads (bright) are arranged in chains and (a) square or (b) hexagonal clusters. Scale bar, 100 μm. χ_f and χ_m denote the magnetic susceptibility of the FF and magnetic beads, respectively.
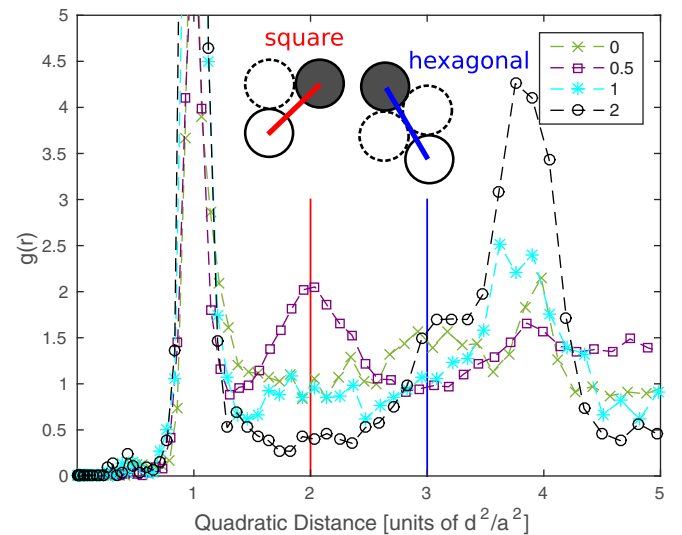
FIG. 3. (Color online) Pair correlation function of pairs of beads, where one is magnetic and one nonmagnetic. Four cases are presented with different effective susceptibilities χ_f/χ_m: 0, 0.5, 1, 2. For the case of low FF susceptibility $\chi_f/\chi_m = 0.5$, a peak is found at the square characteristic distance, and for the high-FF-susceptibility case $\chi_f/\chi_m = 2$, there is a peak at the hexagonal characteristic distance.
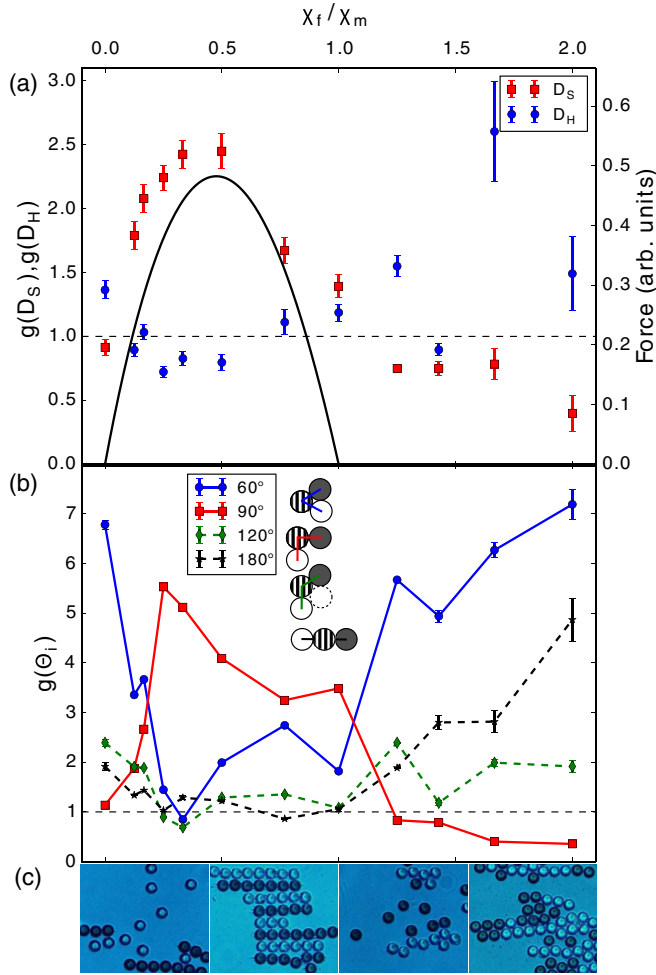
FIG. 4. (Color online) (a) The heights of square (D_S) and hexagonal (D_H) peaks (Fig. 3) plotted for different FF susceptibilities together with the magnetic dipole-dipole force (solid line). (b) The intensity of the angular distribution function at the characteristic angles $60°$, $90°$, $120°$, and $180°$ of one bead with one magnetic and one nonmagnetic nearest-neighbor bead vs FF susceptibility. (c) For four cases (left to right $\chi_f/\chi_m \approx 0.13, 0.5, 1, 1.67$) characteristic images are shown: random arrangement of nonmagnetic beads, square lattice, random arrangement of magnetic beads, hexagonal lattice. The error bars show the standard deviations of the weighted mean values from around 30 images.

Four regions can be distinguished. For each of them a characteristic image is shown [Fig. 4(c)].

IV. DISCUSSION

The characteristic peaks in the radial and angular correlation functions can be seen as a quantitative measure of the degree of ordering in the corresponding phase. The particle interaction in the colloid can be described with the concept of an effective magnetic susceptibility. For beads with diameter on the order of a micrometer, the water with the magnetite nanoparticles can be treated as a homogeneous medium. The beads displace the ferrofluid within their volume and their susceptibility is effectively reduced by the susceptibility of the ferrofluid. This approach is analogous to the Archimedes

principle. The effective magnetic behavior of the beads can be described by point dipoles with magnetic moments [7,8]

$$\widetilde{m}_i = \widetilde{\chi}_i V H_{\text{ext}}, \tag{1}$$

where V is the bead volume and H_{ext} is the external field, and the effective susceptibilities are

$$\widetilde{\chi}_i = 3 \frac{\chi_i - \chi_f}{\chi_i + 2\chi_f + 3}, \tag{2}$$

where χ_i is the particle susceptibility and χ_f is the susceptibility of the ferrofluid. The susceptibility is $\chi_i = \chi_m$ for a magnetic bead and $\chi_i = 0$ for a nonmagnetic bead. The effective magnetic susceptibility of the beads changes with the susceptibility of the FF. In the limit of matched susceptibility of the liquid and particles one obtains zero moments, as expected, and for the limit of zero susceptibility of the liquid one obtains $m = 3 \frac{\chi_m}{\chi_m + 3} V H$, which is what is expected for a magnetic sphere [19].

Four cases can be distinguished, as shown in Fig. 5. First, at $\chi_f = 0$, with water as a solvent only the polystyrene spheres with a magnetite shell are magnetic. Second, for $\chi_f < \chi_m$, with low concentrations $\rho_{\text{vol}} < 0.72\%$ of magnetite nanoparticles the polystyrene spheres get an effective susceptibility of opposite sign to that of beads with magnetite shell. Third, $\chi_f = \chi_m$, with a concentration $\rho_{\text{vol}} \approx 0.72\%$ of magnetite nanoparticles the susceptibility of the magnetic polystyrene spheres is matched and they become effectively nonmagnetic. The initially nonmagnetic spheres now carry an effective moment. Fourth, $\chi_f > \chi_m$, with high concentrations $\rho_{\text{vol}} > 0.72\%$ of magnetite nanoparticles the effective susceptibilities have the same sign for both types of polystyrene sphere.
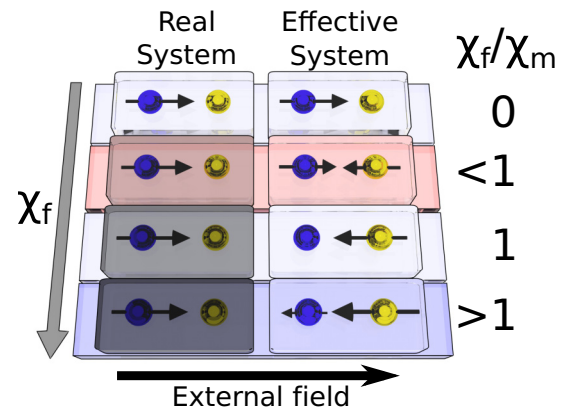
FIG. 5. (Color online) Four cases of absolute and effective susceptibilities for magnetic (blue) and nonmagnetic (yellow) beads can be distinguished: in the real system (from top to bottom) the concentration of the magnetite nanoparticles increases and therefore the susceptibility of the solvent increases. In the effective system the susceptibility of the beads is replaced by effective values and each bead behaves like a point dipole. In this figure the formation of structure can be understood as the minimization of magnetostatic energy between dipoles, where each bead can be seen as a disk with an effective point dipole in the center. For the cases $\chi_f/\chi_m = 0$ and $\chi_f/\chi_m = 1$ only one sort of bead shows magnetic response. In the case $\chi_f/\chi_m < 1$ (red highlighted) the dipole moments are antiparallel to each other and for $\chi_f/\chi_m > 1$ (blue highlighted) they are parallel.
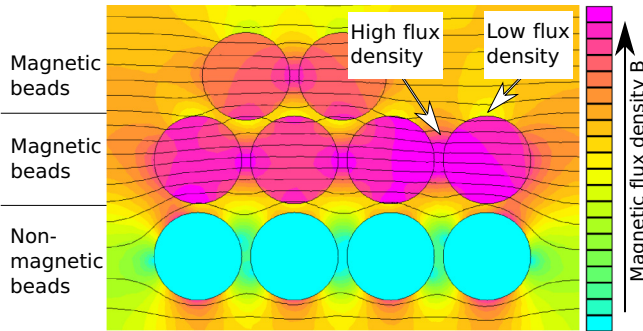
FIG. 6. (Color online) The color map displays the calculated field of a cluster of magnetic and nonmagnetic beads for the case $\chi_f/\chi_m \approx 0.5$: the nonmagnetic beads arrange in areas with low field and the magnetic ones in areas with high field. The field has been calculated with the software FEMM with a finite-element method.

The formation of hexagonal or square lattices is a result of the minimization of the magnetostatic energy of dipole-dipole interactions, where each bead acts as point dipole. For magnetic beads this energy is minimal in areas with high magnetic flux density, whereas for nonmagnetic beads it is minimal in areas with low flux density. The calculated magnetic flux density around a chain of four magnetic beads is shown in Fig. 6. The flux density is high between two magnetic beads and low just beside the chain.

The phase diagram in Fig. 4 is explained by calculation of the magnetic force between the particles. The arrangement of the beads is driven by dipole-dipole interaction. The dipole-dipole force between two beads is proportional to the product of the effective moments and therefore in a constant homogeneous field to the effective susceptibilities

$$f \propto \widetilde{\chi}_i \cdot \widetilde{\chi}_j. \tag{3}$$

The force between magnetic and nonmagnetic beads can be described by the effective susceptibilities from Eq. (2), where the real susceptibilities $\chi_i = \chi_m$ for the magnetic beads and $\chi_j = 0$ for the nonmagnetic beads are inserted. The solid line in Fig. 4(a) displays the scaling of the dipole-dipole force. When the sign of the force changes, the effective magnetization of the magnetic beads is switched from paramagnetic to diamagnetic while the effective magnetization of the nonmagnetic beads remains diamagnetic. This results in a switching from antiparallel to parallel alignment between the magnetic moments of both types. The square structure is favored for antiparallel alignment, while the hexagonal structure is favored for parallel

alignment. Therefore, the change of the sign of the force results in a phase transition. As the magnitude of the force between the beads increases, more beads are found in the corresponding phase, which means that bigger clusters are assembled. The cluster growth is limited by the dynamics of the system. After the initial formation of the clusters the growth rate is very slow. The observed configurations can be seen as dynamically frozen, because the Brownian motion is very slow and the Boltzmann factor is large, $\frac{\Delta E}{k_B T} \approx 10^6$, where ΔE is the interaction energy between two beads, k_B is the Boltzmann constant, and $T = 300$ K is the temperature.

V. CONCLUSION

In the present article we describe a system of magnetic and nonmagnetic colloidal particles dispersed in a magnetic matrix. By changing the magnetic susceptibility of the carrier liquid the interaction between the particles is tuned from antiferromagnetic to ferrimagnetic. This goes in hand with a phase transition from square to hexagonal ordering. Our findings are explained by a minimization of the magnetostatic energy.

The phase diagram is established by a statistical evaluation of transmission microscope images of a sample confined in two dimensions. The statistical approach allows one to access structural information by evaluation of order parameters. This not only opens the door to studying the equilibrium structure but also allows systematic investigations of the dynamics of structure formation and the characterization of frustrated systems. Moreover, our real-space approach allows direct comparison to scattering data after Fourier transformation, which is useful for the investigation of three-dimensional systems.

Apart from the potential for studying the physics of phase formation, the manipulation of self-assembled structures will result in very interesting applications. One example is the use of branching chains in magnetorheological fluids to tune the viscosity in a liquid for specific applications such as adaptable dampers [20], or the self-assembly of metamaterials as plasmonic arrays [21,22] or of photonic crystals [23,24] with novel material properties.

[1] G. M. Whitesides and B. Grzybowski, Science **295**, 2418 (2002).

[2] K. J. M. Bishop, C. E. Wilmer, S. Soh, and B. A. Grzybowski, Small **5**, 1600 (2009).

[3] K. Zhao and T. G. Mason, Phys. Rev. Lett. **99**, 268301 (2007).

[4] V. Kitaev and G. A. Ozin, Adv. Mater. **15**, 75 (2003).

[5] R. Cademartiri, C. A. Stan, V. M. Tran, E. Wu, L. Friar, D. Vulis, L. W. Clark, S. Tricard, and G. M. Whitesides, Soft Matter **8**, 9771 (2012).

[6] A. F. Demirörs, P. M. Johnson, C. M. van Kats, A. van Blaaderen, and A. Imhof, Langmuir **26**, 14466 (2010).

[7] R. Erb, H. Son, B. Samanta, V. Rotello, and B. Yellen, Nature (London) **457**, 999 (2009).

[8] K. Khalil, A. Sagastegui, Y. Li, M. Tahir, J. Socolar, B. Wiley, and B. Yellen, Nat. Commun. **3**, 794 (2012).

[9] D. Du, D. Li, M. Thakur, and S. L. Biswal, Soft Matter **9**, 6867 (2013).

[10] A. V. Straube and P. Tierno, Soft Matter **10**, 3915 (2014).

[11] A. Snezhko, M. Belkin, I. S. Aranson, and W.-K. Kwok, Phys. Rev. Lett. **102**, 118103 (2009).

[12] R. Alert, J. Casademunt, and P. Tierno, Phys. Rev. Lett. **113**, 198301 (2014).

[13] J. Byrom and S. L. Biswal, Soft Matter **9**, 9167 (2013).

[14] A. Yethiraj and A. van Blaaderen, Nature (London) **421**, 513 (2003).

[15] A. Skjeltorp, Physica B+C **127**, 411 (1984).

[16] A. Skjeltorp and G. Helgesen, Physica A **176**, 37 (1991).

[17] S. Merminod, M. Berhanu, and E. Falcon, Europhys. Lett. **106**, 44005 (2014).

[18] Y. Yang, L. Gao, G. P. Lopez, and B. B. Yellen, ACS Nano **7**, 2705 (2013).

[19] B. Bleaney, *Electricity & Magnetism*, 2nd ed. (Oxford University Press, Oxford, 1965).

[20] B. J. Park, F. F. Fang, and H. J. Choi, Soft Matter **6**, 5246 (2010).

[21] L. Jiang, C. Zou, Z. Zhang, Y. Sun, Y. Jiang, W. Leow, B. Liedberg, S. Li, and X. Chen, Small **10**, 609 (2014).

[22] J. A. Fan, C. Wu, K. Bao, J. Bao, R. Bardhan, N. J. Halas, V. N. Manoharan, P. Nordlander, G. Shvets, and F. Capasso, Science **328**, 1135 (2010).

[23] Y. Saado, M. Golosovsky, D. Davidov, and A. Frenkel, Phys. Rev. B **66**, 195108 (2002).

[24] L. He, Y. Hu, H. Kim, J. Ge, S. Kwon, and Y. Yin, Nano Lett. **10**, 4708 (2010).